frontiers | Frontiers in Energy Research

PERSPECTIVE
published: 05 July 2022
doi: 10.3389/fenrg.2022.956444

Solar-Driven Carbon Dioxide Reduction: A Fair Evaluation of Photovoltaic-Biased Photoelectrocatalysis and Photovoltaic-Powered Electrocatalysis

Ying Zhang†, Conglin Ye†, Jingjing Duan, Hao Feng, Dong Liu and Qiang Li**

MIIT Key Laboratory of Thermal Control of Electronic Equipment, School of Energy and Power Engineering, Nanjing University of Science and Technology, Nanjing, China

OPEN ACCESS

Edited by:
Jian Li,
Tsinghua University, China

Reviewed by:
Yongjie Wang,
Harbin Institute of Technology, China
Daniel Tudor Cotfas,
Transilvania University of Braşov, Romania
Yao Zheng,
University of Adelaide, Australia

***Correspondence:**
Dong Liu
liudong15@njust.edu.cn
Qiang Li
liqiang@njust.edu.cn

†These authors have contributed equally to this work and share first authorship

Specialty section:
This article was submitted to Process and Energy Systems Engineering, a section of the journal Frontiers in Energy Research

Received: *30 May 2022*
Accepted: *15 June 2022*
Published: *05 July 2022*

Citation:
Zhang Y, Ye C, Duan J, Feng H, Liu D and Li Q (2022) Solar-Driven Carbon Dioxide Reduction: A Fair Evaluation of Photovoltaic-Biased Photoelectrocatalysis and Photovoltaic-Powered Electrocatalysis. Front. Energy Res. 10:956444. doi: 10.3389/fenrg.2022.956444

The salient question addressed in this work is whether and how photovoltaic-biased photoelectrocatalysis (PV-PEC) can fairly and practically be as competitive as photovoltaic-powered electrocatalysis (PV-EC) for solar-driven carbon dioxide reduction (CO_2RR). It was argued that to fairly evaluate PV-PEC and PV-EC CO_2RR approaches in terms of techno-economy, the two devices should be driven by the same PV cell and produce the same group of products for the same series of Faradaic efficiency for each product. For this condition, PV-PEC CO_2RR was shown to surprisingly have higher solar-to-chemical (STC) energy conversion efficiency than PV-EC. Results show that the STC efficiency of 8%, double the state-of-the-art efficiency, is achievable for PV-PEC CO_2RR that employs low-cost perovskite PV cell and silicon PEC photocathode. This non-trivial performance was achieved by leveraging novel design of light management. In particular, the proposed reflective-spectrum-splitting light management configuration enables the use of high-efficiency opaque perovskite PV cell, which significantly boosts the efficiency of PV-PEC CO_2RR. Furthermore, the framework generalized in this work is also applicable to other solar-driven catalytic processes with various different products such as productions of H_2O_2 by water oxidation and ammonia by nitrogen fixation.

Keywords: solar fuel, CO2 reduction, photoelectrocatalysis, electrocatalysis, techno-economy

INTRODUCTION

Converting carbon dioxide and water into useful chemicals using solar energy offers a means to provide an alternative to fossil fuels and to mitigate global warming (White et al., 2015; Kumaravel et al., 2020). Since approximately 2.6 V voltage is needed for carbon dioxide reduction reaction (CO_2RR), water oxidation reaction and corresponding overpotentials (White et al., 2015), no single semiconductor can provide such a high voltage except for those having wide band gaps and thereby absorbing solar energy over a very narrow spectrum. Therefore, a photovoltaic (PV) cell that provides an extra bias, can be coupled to a photoelectrocatalysis (PEC) cell comprising a semiconductor photocathode for CO_2RR and a counter electrode for water oxidation. CO_2RR devices that use the photovoltaic-biased photoelectrocatalysis (PV-PEC) approach (Gurudayal et al.,

2019), have shown higher solar-to-chemical (STC) energy conversion efficiency compared to those use photocatalysis (Sorcar et al., 2019). Ager and his colleagues (Gurudayal et al., 2019) reported the state-of-the-art STC efficiency of 3.5% for PV-PEC CO_2RR that produced C_{2+} products; while the efficiency for photocatalysis CO_2RR was as low as 1% reported by Sorcar et al. (Sorcar et al., 2019) where methane and ethane were produced. A PV cell can also power an electrocatalysis (EC) cell to construct a PV-EC CO_2RR device, which is thought to be technologically more mature (Gurudayal et al., 2017; Schreier et al., 2017; Wang et al., 2018; Chen et al., 2019; Huan et al., 2019; Zhou et al., 2019; Cheng et al., 2020; Kim et al., 2020; Kumaravel et al., 2020; Xiao et al., 2020). By using III-V multi-junction solar cells and noble metal-based catalysts, the STC efficiency of ~20% has been demonstrated for PV-EC CO_2RR that produced carbon monoxide (Cheng et al., 2020; Xiao et al., 2020). For PV-EC CO_2RR that produces C_{2+} products, the state-of-the-art STC efficiency is 8.4% reported by Gurudayal et al. (Gurudayal et al., 2017) where III-V multi-junction solar cell was used, and is ~5.2% reported by Huan et al. (Huan et al., 2019) where perovskite solar cell was used.

Longstanding debate goes for and against PV-PEC versus PV-EC. For PV-PEC and PV-EC CO_2RR devices, the solar-to-chemical energy conversion efficiency, η_{STC}, is expressed as (White et al., 2015)

$$\eta_{STC} = \frac{J_{op} \times \sum_i \left(FE_i \times E_i^0\right)}{P_{in}} \quad (1)$$

where P_{in} is the incident solar power, FE_i and E_i^0 are the Faradaic efficiency and the thermodynamic potential of product i, and J_{op} is the operating current density of the device. The operating condition is determined as the cross point of the current density-voltage (J-V) curve of the PV cell and the J-V curve of the PEC or EC cells. Since the summation of the voltage produced by the photocathode and that by the PV cell, provides the necessary device voltage for PV-PEC, the PV cell in PV-PEC provides a smaller voltage than that in PV-EC, thereby generating a larger current density. Thus, a PV-PEC device has potentially higher η_{STC} than PV-EC according to **Eq. 1**. However, for devices that use low-cost perovskite solar cells and produce C_{2+} products, the state-of-the-art STC efficiency for PV-PEC CO_2RR is 3.5% (Gurudayal et al., 2019) which is lower than the efficiency of ~5.2% for PV-EC (Huan et al., 2019). These efficiency numbers contradict what **Eq. 1** tells and skepticism has grown regarding PV-PEC as an alternative to PV-EC (Jacobsson, 2018). Therefore, the core question addressed in this work is whether PV-PEC CO_2RR can practically be as competitive as PV-EC, and how.

CONCEPT

We believe that the comparison of the efficiency numbers without any prerequisites is not fair to evaluate PV-PEC and PV-EC CO_2RR approaches; and thus, we proposed a new method to fairly compare their performance.

Let us revisit the STC efficiency of a PV-EC CO_2RR device. It can always operate at the maximum power point of the PV cell by 1) using a power management unit (shown in **Figure 1A**), 2) adjusting the area ratios of PV cell to the PEC cell (Schreier et al., 2017) or 3) connecting more or fewer EC cells to the PV cell. Therefore, the STC efficiency of a PV-EC CO_2RR device, $\eta_{PV\text{-}EC}$, is expressed as

$$\eta_{PV-EC} = \eta_{PV} \times \frac{1}{V_{op}} \times \sum_i \left(FE_i \times E_i^0\right) \quad (2)$$

where η_{PV} is the solar-to-electricity conversion efficiency of the PV cell and V_{op} is the operating voltage of the EC cell. **Eq. 2** shows that, to fairly compare the performance of PV-EC and PV-PEC CO_2RR devices, they should be driven by the same PV cell (corresponding to the first term in **Eq. 2**, η_{PV}); and the PV-EC CO_2RR device should operate at such V_{op} (corresponding to the second term, $1/V_{op}$) that PV-EC and PV-PEC CO_2RR devices produce the same group of products for the same series of Faradaic efficiency for each product (corresponding to the third term, $\sum(FE_i \times E_i^0)$).

Noteworthy, these prerequisites are self-consistent in terms of techno-economy. A comprehensive economic comparison of these two technologies, which are still under development, may be speculative and is beyond the scope of this work. However, it is interesting to perform a thought experiment. Let us take the product price divided by the device cost as the measure (Jacobsson et al., 2014). CO_2RR products have various profitability (Singh et al., 2015), so the product prices of PV-PEC and PV-EC CO_2RR devices match if they produce the same group of products for the same series of Faradaic efficiency for each product. Their device costs, a large portion of which comes from the PV cell, are also comparable to each other if they are driven by the same PV cell. Therefore, for this condition, the approach with higher STC efficiency is more competitive.

More insights can be given into **Eq. 2**. First, it tells that $\eta_{PV\text{-}EC}$ can be easily enhanced by using III-V multi-junction solar cells with high η_{PV}. However, the cost of this type of solar cells is very high; and thus, they are not practical for large scale applications. This also demonstrates that driven by the same PV cell is a necessary prerequisite to fairly compare PV-EC and PV-PEC CO_2RR. Secondly, the same catalyst (usually metallic nanostructures) can be used for both the cathode in a PV-EC CO_2RR device, but also the co-catalyst of the photocathode in the counterpart PV-PEC CO_2RR device (shown in **Figure 1B**). This is a specific feature of CO_2RR where high loading of metal co-catalyst nanoparticles or other nanostructures are required to increase selectivity to CO_2RR and to decrease H_2 production (Song et al., 2017), and as a result dominate the electrolysis properties of the photocathode (Gurudayal et al., 2019). Thus, PV-EC and the counterpart PV-PEC CO_2RR devices will produce the same group of products for the same series of Faradaic efficiency for each product, if they operate at the same current density, *i.e.,* the working voltage of the metallic catalyst is equal to the summation of the voltage produced by the photocathode and that by the PV cell (Beranek, 2019). Therefore, our proposed comparison method is fair and viable.

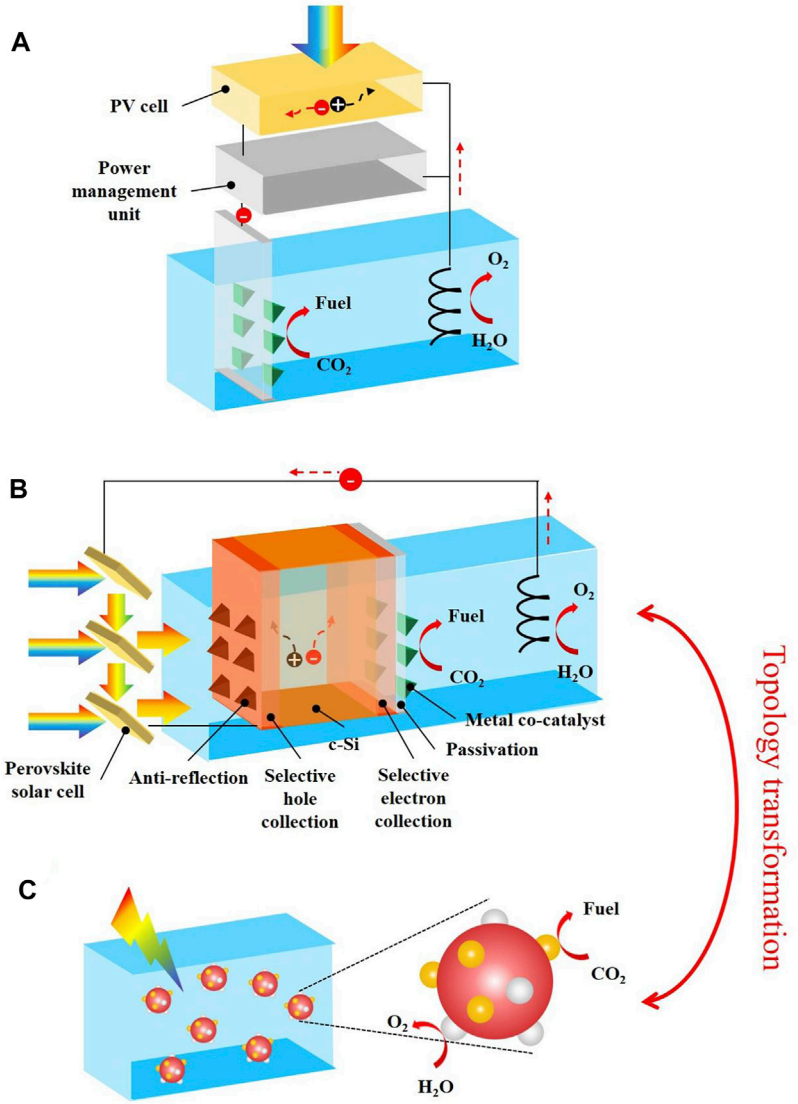

FIGURE 1 | Solar-driven CO2RR approaches investigated in this work. **(A)** PV-EC CO2RR with a power management unit. **(B)** PV-PEC CO2RR with the device architecture designed in this work. **(C)** CO2RR using suspended semiconductor nanoparticles with two different co-catalysts deposited on the surface, which is topologically transformed from PEC CO2RR.

PROOF-OF-CONCEPT

In the first step, careful management of light and choice of PV and PEC cells were presented for PV-PEC CO_2RR to enhance its STC efficiency and resultantly improve its competitiveness. In a PV-PEC device both PV and PEC cells absorb sunlight, from separated spectra though, and they overlap each other sharing the same area, unlike the configuration of a PV-EC device where only the PV cell absorbs light. In addition, although the overall voltage is the sum of the voltages of these 2 cells, the operating current density is limited by the smaller one determined by sunlight absorption of each cell. Therefore, the optical coupling between PV and PEC cells must be carefully optimized to enhance η_{STC} according to **Eq. 1**. Toward this end, guided by careful light management, we proposed the PV-PEC CO_2RR device architecture shown in **Figure 1B** with following features. 1) sunlight is illuminated from the un-reaction side of the photocathode. As mentioned above, high loading of metal co-catalyst is required to increase CO_2RR selectivity. This co-catalyst layer has very low optical transmission (Jang et al., 2016; Song et al., 2017; Hu et al., 2018) compared to the co-catalyst layer of photoelectrode for water splitting (usually higher than 90% (Abdi et al., 2013), see **Supplementary Figure S1** for the architecture of a typical PV-PEC water splitting device). Thus, sunlight absorption in the semiconductor absorber, the photocurrent density and the resultant η_{STC} according to **Eq. 1**, would be reduced in a reaction-side-illumination architecture compared to the un-reaction-side-illumination one. 2) The PV cell is in front

of the PEC cell so that the PV cell is not blocked by optically thick metal co-catalyst layer and thereby absorbs enough sunlight. 3) As a result, the semiconductor material in the PEC cell has a narrower band gap than that in the PV cell so that the back PEC cell can absorb sunlight below the band gap wavelength of the semiconductor material in the front PV cell.

More insights can be given into the proposed architecture. The first is given to the semiconductor material used for the PEC cell. An anti-reflection layer is needed on the illumination side to maximize optical absorption. A selective hole collection layer on the illumination side, and a selective electron collection layer and a surface passivation layer on the reaction side, are also needed to promote charge carrier separation and transport. This analysis leads to our choice of crystalline silicon (c-Si), a mature narrow band gap semiconductor in industry, for scale-up, because commercial techniques can be used for c-Si processing including anti-reflection, doping, and passivation. The second is the solar cell. Since c-Si photocathode can provide a photo-voltage of about 0.6 V (Green et al., 2019; Gurudayal et al., 2019), the solar cell must provide the rest 2.0 V to achieve the target voltage of 2.6 V. This leads to our choice of two perovskite solar cells connected in series because they have suitable band gaps, high open circuit voltages and can be fabricated using potentially low cost methods (Green et al., 2019). Usually, semi-transparent perovskite solar cells should be used so that sunlight below their band gap wavelength can be transmitted to the c-Si photocathode. However, the efficiency of semi-transparent perovskite solar cells has been much lower compared to their opaque counterparts. For example, the reported efficiency of the semi-transparent perovskite solar cell in Gurudayal et al. (Gurudayal et al., 2019) is as low as 8.4% (V_{oc} = 1.06 V, J_{sc} = 14.5 mA cm^{-2}, FF = 0.55). Hence, we proposed the reflective-spectrum-splitting light management configuration so that high-efficiency opaque perovskite solar cells can be used for PV-PEC CO_2RR. As shown in **Figure 1B**, this configuration, inspired by window blinds (Liu et al., 2016; Liu and Li, 2017; Zheng et al., 2019), features an array of solar cell panels comprising one side coated by perovskite solar cell and another specular reflective side, or with perovskite solar cells on both sides, so sunlight below their band gap wavelength is not transmitted, but reflected to the c-Si photocathode; and thus, state-of-the-art opaque planar perovskite solar cells can be used. For example, the perovskite solar cell reported in our recent work (Zheng et al., 2019), was used later for theoretical predictions of STC efficiency. The efficiency of this solar cell is as high as 16.7%, which is twice the efficiency of the previous semi-transparent solar cell. So far, it is noteworthy that the proposed PV-PEC CO_2RR device (**Figure 1B**) is totally different from diverse devices reported in literature (Abdi et al., 2013; Jang et al., 2015; Jang et al., 2016; Rothschild and Dotan, 2017; Song et al., 2017; Young et al., 2017; Hu et al., 2018; Gurudayal et al., 2019; Li et al., 2019; Kan et al., 2020; Kempler et al., 2020; Zhang et al., 2020; Liu et al., 2021a; Dong et al., 2021).

In the next step, let us compare the performance of PV-PEC CO_2RR and its counterpart PV-EC CO_2RR. η_{STC} is determined by **Eq. 1** where the current density-voltage (J-V) curves of both PV and PEC/EC cells are needed. The J-V curve of the PV cell can be approximated by the ideal diode equation (Rothschild and Dotan, 2017) expressed as

$$J = J_{sc} - J_0\left[\exp\left(\frac{qV}{kT}\right) - 1\right] \quad (3)$$

where experimental short-circuit current density (J_{sc} = 19.00 mA cm^{-2}) and open-circuit voltage (V_{oc} = 1.19 V) reported in a recent work by our group (Zheng et al., 2019) for a single perovskite solar cell (1.66 eV band gap) are the input parameters. For two perovskite solar cells connected in series, J_{sc} will be reduced by a factor of two with V_{oc} being doubled. The black dashed curve in **Figure 2A** shows the J-V curve of two of these perovskite solar cells connected in series. This perovskite solar cell was chosen for three reasons. 1) It employs planar structure which is a requisite for the reflective spectrum splitting configuration. 2) Two of these perovskite solar cells connected in series can produce high V_{oc} of 2.38 V 3) They can also produce J_{sc} of 9.50 mA cm^{-2} rendering η_{STC} higher than 10% corresponding to **Eq. 1**.

The two-electrode J-V curve of the PEC cell with the photocathode comprising a c-Si photoabsorber and a high loading of metal co-catalyst, can be calculated from the measured J-V behavior of a c-Si photoabsorber for light condition and the measured two-electrode J-V curve of an electrocatalysis cell using a metallic cathode for dark condition (Coridan et al., 2015; Zhou et al., 2016), because the electrolysis properties of the photocathode were dominated by the metal co-catalyst, and resultantly, the light harvesting process of the c-Si photoabsorber and the electrolysis process of the metal co-catalyst are decoupled from each other. As mentioned above, the same metal catalyst is used for both the photocathode in PV-PEC CO_2RR but also the cathode in the counterpart PV-EC CO_2RR, so we took the results for the nanostructured Cu-Ag bimetallic catalyst reported in Gurudayal et al. (Gurudayal et al., 2017) as an example. The cathode employing this catalyst showed high selectivity to the production of hydrocarbons and oxygenates that can exploit existing infrastructures. Moreover, its required voltage at the current density of ~10 mA cm^{-2} can be provided by the summation of the photo-voltages generated from the PV cell and the c-Si photoabsorber. When this Cu-Ag catalyst is loaded on the photocathode surface, the product distribution of PEC should be similar to that of EC where the catalyst works by itself; at the same time, the operating potential of PEC is positively shifted due to the photo-voltage from the photocathode. The J-V behavior of the c-Si photoabsorber for light condition was also approximated by the ideal diode equation (see **Supplementary Figure S2**). In the proposed architecture (**Figure 1B**), the PV cell is in front of the PEC cell, so the back c-Si photoabsorber receives less sunlight and thus, generates smaller J_{sc}. The perovskite solar cell absorbs sunlight below 747 nm (1.66 eV), thereby reducing the J_{sc} of the c-Si photoabsorber by 55%. Therefore, the input parameters into the diode equation are experimental short-circuit current density (30 mA cm^{-2}) reduced by 55% and open-circuit voltage (0.6 V) reported for the c-Si photoabsorber (Gurudayal et al., 2019). The measured two-electrode J-V curve of an electrocatalysis cell using the Cu-Ag catalyst cathode for dark

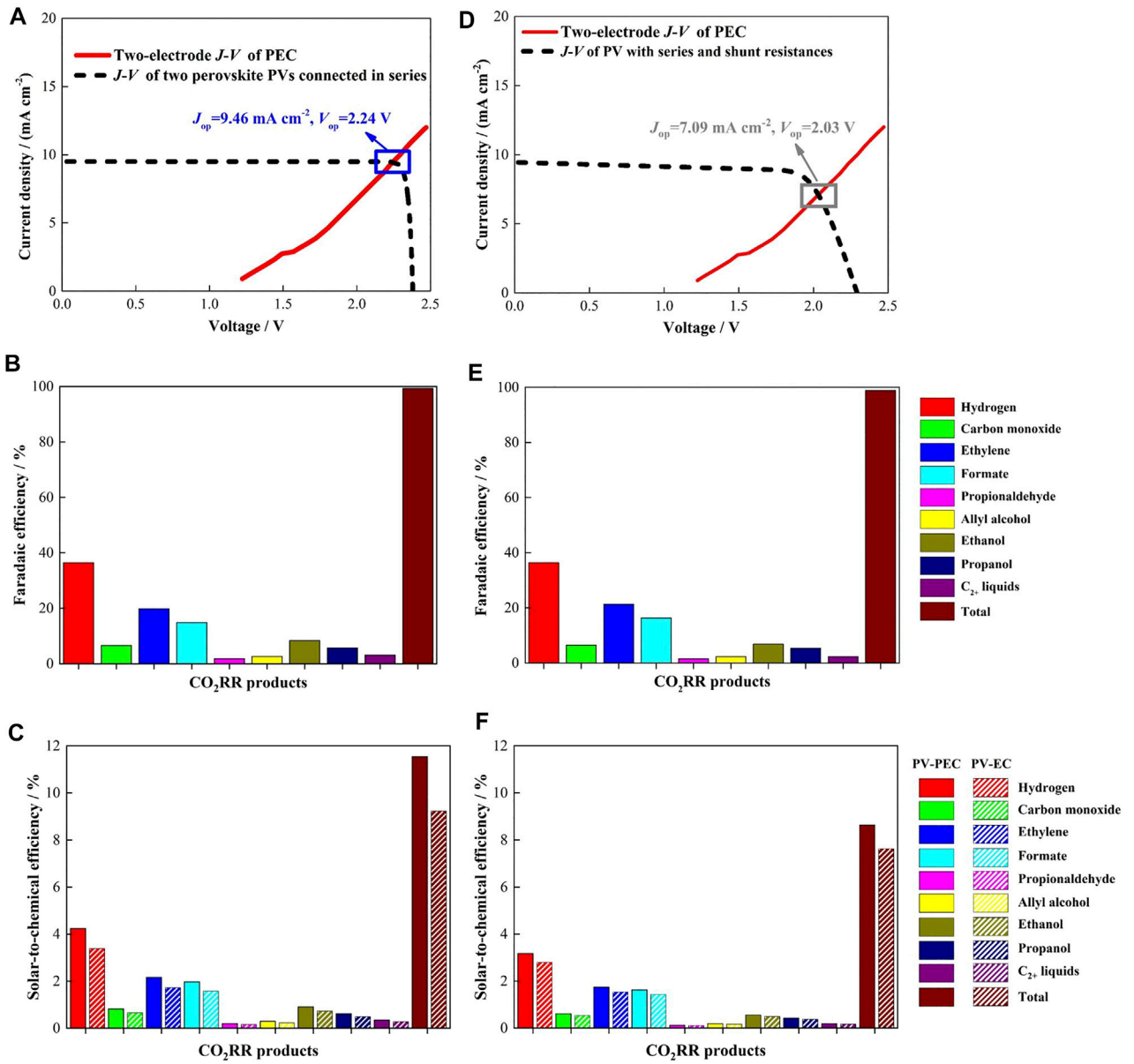

FIGURE 2 | Performance of PV-PEC CO_2RR and the counterpart PV-EC CO_2RR. **(A)** *J-V* curve of two perovskite solar cells connected in series and two-electrode *J-V* curve of PEC cell with the photocathode comprising a c-Si photoabsorber and a high loading of nanostructured Cu-Ag bimetallic co-catalyst. **(B)** Faradaic efficiency of each product for both PV-PEC CO_2RR and the counterpart PV-EC corresponding to the operating point (the operating point for PV-EC was obtained from **Supplementary Figure S2**). They have the same product distribution. **(C)** STC efficiency of PV-PEC CO_2RR and the counterpart PV-EC for each product and all products. The values were calculated using **Eq. 1** for PV-PEC and **Eq. 2** for PV-EC. Input parameters for **Eqs 1**, **2** were obtained from **Figures 2A,B**. **(D)–(F)** Achievable STC efficiency of PV-PEC CO_2RR. In this case, **Eq. 4** was used to describe the PV cell and the input parameters for **Eqs 1**, **2** were obtained from **Figures 2D,E**. PV-PEC CO_2RR still has higher STC efficiency than PV-EC because they are driven by the same PV cell.

condition was taken from Gurudayal et al. (Gurudayal et al., 2017) (see **Supplementary Figure S2**). Then, the two-electrode *J-V* curve of the PEC cell with the photocathode comprising a c-Si photoabsorber and a high loading of nanostructured Cu-Ag bimetallic co-catalyst was calculated and shown as the red curve in **Figure 2A**.

This model device of PV-PEC CO_2RR operates at 9.46 mA cm^{-2} and 2.24 V as shown in **Figure 2A**. The corresponding Faradaic efficiency of each product shown in **Figure 2B** was obtained from Gurudayal et al. (Gurudayal et al., 2017). This operating condition is very close to the maximum power point of the PV cell as a result of novel light management and careful cell choice. The solar-to-chemical conversion efficiency, $\eta_{PV\text{-}PEC}$, was calculated using **Eq. 1**. STC efficiency for each product was shown in **Figure 2C** with their thermodynamic potential listed in **Supplementary Table S1**

(Gurudayal et al., 2017). STC efficiency for all products is as high as 11.5% with a notable efficiency of 6.5% for producing hydrocarbons and oxygenates. Then, STC efficiency of the counterpart PV-EC CO_2RR device was calculated from **Eq. 2**. $\eta_{PV} = 21.3\%$ was obtained from the *J-V* curve of the PV cell shown in **Figure 2A**. V_{op} = 2.81 V, which corresponds to the current density of 9.46 mA cm^{-2}, was obtained from the two-electrode *J-V* curve of the EC cell shown in **Supplementary Figure S2**. The Faradaic efficiency of each product was the same as that of PV-PEC CO_2RR device shown in **Figure 2B**. The calculated STC efficiency of this counterpart device, which is driven by the same two perovskite solar cells connected in series, was also shown in **Figure 2C**. Noteworthy, $\eta_{PV\text{-}EC}$ for all products is 9.2%, which is lower than $\eta_{PV\text{-}PEC}$ of 11.5%. These results demonstrate the competitiveness of PV-PEC CO_2RR comparable to PV-EC CO_2RR. Again, this non-trivial performance, which has never been demonstrated before, is attributed to our novel design of light management and careful choice of both the PV and PEC cells.

DISCUSSION

Achievable STC efficiency of our proposed PV-PEC CO_2RR device. Besides the light management, the gap between the measure STC efficiency in literature and the theoretical predictions in this work is also caused by the performance of the photoabsorber of the photocathode and the performance of the PV cell. In previous analyses, the *J-V* behavior of the c-Si photoabsorber was approximated by the ideal diode equation (**Eq. 3**). Its performance, however, will be reduced by the non-ideal series and shunt resistances. Therefore, we use the following equation (Fountaine et al., 2016),

$$V = \frac{kT}{q}\ln\left[\frac{J_{sc} - J - (V + JR_s)/R_{sh}}{J_0} + 1\right] - JR_s, \qquad (4)$$

to describe c-Si photoabsorber. The input parameters are V_{oc} = 0.6 V, J_{sc} = 13.5 mA cm^{-2}, R_s = 0.1 Ω cm^{-2} and R_{sh} = 5 × 10^7 Ω cm^{-2}. These parameters have been experimentally validated (Gurudayal et al., 2019). The obtained result was then used to calculate the two-electrode *J-V* curve of the PEC cell. Figure S3 shows that the operating point and resultantly, the STC efficiency are nearly identical to those predicted using **Eq. 3**. These results are expected because mature techniques have been developed for the processing of c-Si, and both R_s = 0.1 Ω cm^{-2} and R_{sh} = 5 × 10^7 Ω cm^{-2} are high-quality values.

The *J-V* curve of the perovskite solar cell was also approximated by the ideal diode equation in previous analyses, so again, we use **Eq. 4** to describe this solar cell. The input parameters are V_{oc} = 1.146 V, J_{sc} = 19.0 mA cm^{-2}, R_s = 6.2 Ω cm^{-2} and R_{sh} = 926 Ω cm^{-2}. Specifically, these realistic parameters are for inclined illumination with an incident angle of 45° (Zheng et al., 2019), which is required by the reflective spectrum splitting configuration. **Figure 2D** shows that the non-ideal series and shunt resistances decrease the fill factor of the PV cell; as a result, the operating current density of PV-PEC CO_2RR device is reduced to 7.09 mA cm^{-2}. The corresponding Faradaic efficiency of each product is shown in **Figure 2E** with the resultant STC efficiency shown in **Figure 2F**. The STC efficiency for all products is reduced to 8.6%, which is ~2.4 times the value reported in Gurudayal et al. (Gurudayal et al., 2019). Since our proposed light management strategy allows the integration of opaque perovskite solar cell with an efficiency twice the efficiency of the semi-transparent perovskite solar cell used in Gurudayal et al. (Gurudayal et al., 2019), we believe the STC efficiency of ~8% is achievable for PV-PEC CO_2RR.

Perspectives on the scale-up of our proposed PV-PEC CO_2RR device. First, the preparation of the photocathode shown in **Figure 1B** could use the following steps. 1) Texturing silicon wafer on both sides. This could be done with conventional chemical etching methods. 2) Preparing the selective charge carrier collection layers. The ion implantation method could be used to perform n^+ doping for the preparation of the selective electron collection layer on the reaction side, and p^+ doping for the selective hole collection layer on the illumination side. 3) Preparation of the passivation coating. The vapour deposition and atomic-layer deposition (ALD) methods could be used to prepare a thin oxide coating (TiO_2, SiO_2, Al_2O_3, etc.) to passivate the silicon surface. 4) Fabrication of the metallic co-catalyst layer. This could be done with vapour deposition and electrodeposition methods. Notably, all these steps could be performed using commercial techniques. Secondly, the stability of the photocathode is also important for scale-up (Hu et al., 2015; Kumaravel et al., 2020; Liu et al., 2021b). Studies have shown that the passivation coating of oxide thin films, especially TiO_2 films prepared by ALD, can also effectively protect photocathodes made of non-oxide materials (silicon in this work), and efficiently transport electrons to the co-catalyst layer (Hu et al., 2015).

Outlook. In this work, the advantage of PV-PEC over PV-EC has been demonstrated for solar-driven CO_2RR in terms of techno-economy. This advantage was enabled by novel design of light management. We must further emphasize that the framework generalized in this work is also applicable to other solar-driven catalytic processes with various different products such as productions of H_2O_2 by water oxidation and ammonia by nitrogen fixation (Liu et al., 2019; Xue et al., 2019). Moreover, PEC can be topologically transformed to the approach of suspended semiconductor nanoparticles with two different co-catalysts deposited on the surface (shown in **Figure 1C**) (Tilley, 2019), rendering it a much cheaper technology. Therefore, this work, in combination with a previous viewpoint demonstrating the advantage of PEC in terms of selectivity (Beranek, 2019), motivates PEC investigations, a less explored area, for high-performance solar-driven catalytic technologies.

DATA AVAILABILITY STATEMENT

The original contributions presented in the study are included in the article/**Supplementary Material**, further inquiries can be directed to the corresponding authors.

AUTHOR CONTRIBUTIONS

YZ, CY, and DL conceived the project. YZ, CY, JD, and HF performed the theoretical work. DL and QL provided the framework and directed the project. All authors contributed to the article and approved the submitted version.

FUNDING

This work was supported by National Natural Science Foundation of China (Grant Nos. 51888103, 52006103, 51976090, and 52006101), Scientific and Technological Innovation Project of Carbon Emission Peak and Carbon Neutrality of Jiangsu Province (No. BE2022024), Natural Science Foundation of Jiangsu Province (Nos. BK20200072, BK20200491, and BK20200500) and China Postdoctoral Science Foundation (No. 2020M681603).

SUPPLEMENTARY MATERIAL

The Supplementary Material for this article can be found online at: https://www.frontiersin.org/articles/10.3389/fenrg.2022.956444/full#supplementary-material

REFERENCES

Abdi, F. F., Han, L., Smets, A. H. M., Zeman, M., Dam, B., and Van De Krol, R. (2013). Efficient Solar Water Splitting by Enhanced Charge Separation in a Bismuth Vanadate-Silicon Tandem Photoelectrode. *Nat. Commun.* 4, 2195. doi:10.1038/ncomms3195

Beranek, R. (2019). Selectivity of Chemical Conversions: Do Light-Driven Photoelectrocatalytic Processes Hold Special Promise? *Angew. Chem. Int. Ed.* 58, 2–8. doi:10.1002/anie.201908654

Chen, P., Jiao, Y., Zhu, Y.-H., Chen, S.-M., Song, L., Jaroniec, M., et al. (2019). Syngas Production from Electrocatalytic CO2 Reduction with High Energetic Efficiency and Current Density. *J. Mat. Chem. A* 7, 7675–7682. doi:10.1039/c9ta01932d

Cheng, W. H., Richter, M. H., Sullivan, I., Larson, D. M., Xiang, C., Brunschwig, B. S., et al. (2020). CO_2 Reduction to CO with 19% Efficiency in a Solar-Driven Gas Diffusion Electrode Flow Cell under Outdoor Solar Illumination. *ACS Energy Lett.* 5, 470–476. doi:10.1021/acsenergylett.9b02576

Coridan, R. H., Nielander, A. C., Francis, S. A., McDowell, M. T., Dix, V., Chatman, S. M., et al. (2015). Methods for Comparing the Performance of Energy-Conversion Systems for Use in Solar Fuels and Solar Electricity Generation. *Energy Environ. Sci.* 8, 2886–2901. doi:10.1039/c5ee00777a

Dong, W. J., Navid, I. A., Xiao, Y., Lim, J. W., Lee, J.-L., and Mi, Z. (2021). CuS-Decorated GaN Nanowires on Silicon Photocathodes for Converting CO2 Mixture Gas to HCOOH. *J. Am. Chem. Soc.* 143, 10099–10107. doi:10.1021/jacs.1c02139

Fountaine, K. T., Lewerenz, H. J., and Atwater, H. A. (2016). Efficiency Limits for Photoelectrochemical Water-Splitting. *Nat. Commun.* 7, 13706. doi:10.1038/ncomms13706

Green, M. A., Dunlop, E. D., Levi, D. H., Hohl-Ebinger, J., Yoshita, M., and Ho-Baillie, A. W. Y. (2019). Solar Cell Efficiency Tables (Version 54). *Prog. Photovolt. Res. Appl.* 27, 565–575. doi:10.1002/pip.3171

Gurudayal, G., Beeman, J. W., Bullock, J., Wang, H., Eichhorn, J., Towle, C., et al. (2019). Si Photocathode with Ag-Supported Dendritic Cu Catalyst for CO2reduction. *Energy Environ. Sci.* 12, 1068–1077. doi:10.1039/c8ee03547d

Gurudayal, G., Bullock, J., Srankó, D. F., Towle, C. M., Lum, Y., Hettick, M., et al. (2017). Efficient Solar-Driven Electrochemical CO2 Reduction to Hydrocarbons and Oxygenates. *Energy Environ. Sci.* 10, 2222–2230. doi:10.1039/c7ee01764b

Hu, S., Lewis, N. S., Ager, J. W., Yang, J., McKone, J. R., and Strandwitz, N. C. (2015). Thin-film Materials for the Protection of Semiconducting Photoelectrodes in Solar-Fuel Generators. *J. Phys. Chem. C* 119, 24201–24228. doi:10.1021/acs.jpcc.5b05976

Hu, Y., Chen, F., Ding, P., Yang, H., Chen, J., Zha, C., et al. (2018). Designing Effective Si/Ag Interface via Controlled Chemical Etching for Photoelectrochemical CO2 Reduction. *J. Mat. Chem. A* 6, 21912–21906. doi:10.1039/c8ta05420g

Huan, T. N., Dalla Corte, D. A., Lamaison, S., Karapinar, D., Lutz, L., Menguy, N., et al. (2019). Low-cost High-Efficiency System for Solar-Driven Conversion of CO 2 to Hydrocarbons. *Proc. Natl. Acad. Sci. U.S.A.* 116, 9735–9740. doi:10.1073/pnas.1815412116

Jacobsson, T. J., Fjällström, V., Edoff, M., and Edvinsson, T. (2014). Sustainable Solar Hydrogen Production: from Photoelectrochemical Cells to PV-Electrolyzers and Back Again. *Energy Environ. Sci.* 7, 2056–2070. doi:10.1039/c4ee00754a

Jacobsson, T. J. (2018). Photoelectrochemical Water Splitting: an Idea Heading towards Obsolescence? *Energy Environ. Sci.* 11, 1977–1979. doi:10.1039/c8ee00772a

Jang, Y. J., Jang, J.-W., Lee, J., Kim, J. H., Kumagai, H., Lee, J., et al. (2015). Selective CO Production by Au Coupled ZnTe/ZnO in the Photoelectrochemical CO2 Reduction System. *Energy Environ. Sci.* 8, 3597–3604. doi:10.1039/c5ee01445j

Jang, Y. J., Jeong, I., Lee, J., Lee, J., Ko, M. J., and Lee, J. S. (2016). Unbiased Sunlight-Driven Artificial Photosynthesis of Carbon Monoxide from CO2 Using a ZnTe-Based Photocathode and a Perovskite Solar Cell in Tandem. *ACS Nano* 10, 6980–6987. doi:10.1021/acsnano.6b02965

Kan, M., Yan, Z. W., Wang, X., Hitt, J. L., Xiao, L., McNeill, J. M., et al. (2020). 2-Aminobenzenethiol-Functionalized Silver-Decorated Nanoporous Silicon Photoelectrodes for Selective CO 2 Reduction. *Angew. Chem. Int. Ed.* 59, 11462–11469. doi:10.1002/anie.202001953

Kempler, P. A., Richter, M. H., Cheng, W.-H., Brunschwig, B. S., and Lewis, N. S. (2020). Si Microwire-Array Photocathodes Decorated with Cu Allow CO2 Reduction with Minimal Parasitic Absorption of Sunlight. *ACS Energy Lett.* 5, 2528–2534. doi:10.1021/acsenergylett.0c01334

Kim, B., Seong, H., Song, J. T., Kwak, K., Song, H., Tan, Y. C., et al. (2020). Over a 15.9% Solar-To-CO Conversion from Dilute CO_2 Streams Catalyzed by Gold Nanoclusters Exhibiting a High CO_2 Binding Affinity. *ACS Energy Lett.* 5, 749–757. doi:10.1021/acsenergylett.9b02511

Kumaravel, V., Bartlett, J., and Pillai, S. C. (2020). Photoelectrochemical Conversion of Carbon Dioxide (CO2) into Fuels and Value-Added Products. *ACS Energy Lett.* 5, 486–519. doi:10.1021/acsenergylett.9b02585

Li, C., Wang, T., Liu, B., Chen, M., Li, A., Zhang, G., et al. (2019). Photoelectrochemical CO2 Reduction to Adjustable Syngas on Grain-Boundary-Mediated A-Si/TiO2/Au Photocathodes with Low Onset Potentials. *Energy Environ. Sci.* 12, 923–928. doi:10.1039/c8ee02768d

Liu, D., and Li, Q. (2017). Sub-nanometer Planar Solar Absorber. *Nano Energy* 34, 172–180. doi:10.1016/j.nanoen.2017.02.027

Liu, D., Yu, H., Duan, Y., Li, Q., and Xuan, Y. (2016). New Insight into the Angle Insensitivity of Ultrathin Planar Optical Absorbers for Broadband Solar Energy Harvesting. *Sci. Rep.* 6, 32515. doi:10.1038/srep32515

Liu, G., Narangari, P. R., Trinh, Q. T., Tu, W., Kraft, M., Tan, H. H., et al. (2021a). Manipulating Intermediates at the Au-TiO2 Interface over InP Nanopillar Array for Photoelectrochemical CO2 Reduction. *ACS Catal.* 11, 11416–11428. doi:10.1021/acscatal.1c02043

Liu, G., Zheng, F., Li, J., Zeng, G., Ye, Y., Larson, D. M., et al. (2021b). Investigation and Mitigation of Degradation Mechanisms in Cu2O Photoelectrodes for CO2 Reduction to Ethylene. *Nat. Energy* 6, 1124–1132. doi:10.1038/s41560-021-00927-1

Liu, J., Zou, Y., Jin, B., Zhang, K., and Park, J. H. (2019). Hydrogen Peroxide Production from Solar Water Oxidation. *ACS Energy Lett.* 4, 3018–3027. doi:10.1021/acsenergylett.9b02199

Rothschild, A., and Dotan, H. (2017). Beating the Efficiency of Photovoltaics-Powered Electrolysis with Tandem Cell Photoelectrolysis. *ACS Energy Lett.* 2, 45–51. doi:10.1021/acsenergylett.6b00610

Schreier, M., Héroguel, F., Steier, L., Ahmad, S., Luterbacher, J. S., Mayer, M. T., et al. (2017). Solar Conversion of CO2 to CO Using Earth-Abundant Electrocatalysts Prepared by Atomic Layer Modification of CuO. *Nat. Energy* 2, 17087. doi:10.1038/nenergy.2017.87

Singh, M. R., Clark, E. L., and Bell, A. T. (2015). Thermodynamic and Achievable Efficiencies for Solar-Driven Electrochemical Reduction of Carbon Dioxide to Transportation Fuels. *Proc. Natl. Acad. Sci. U. S. A.* 112, E6111–E6118. doi:10.1073/pnas.1519212112

Song, J. T., Ryoo, H., Cho, M., Kim, J., Kim, J.-G., Chung, S.-Y., et al. (2017). Nanoporous Au Thin Films on Si Photoelectrodes for Selective and Efficient Photoelectrochemical CO2Reduction. *Adv. Energy Mat.* 7, 1601103. doi:10.1002/aenm.201601103

Sorcar, S., Hwang, Y., Lee, J., Kim, H., Grimes, K. M., Grimes, C. A., et al. (2019). CO_2, Water, and Sunlight to Hydrocarbon Fuels: a Sustained Sunlight to Fuel (Joule-To-Joule) Photoconversion Efficiency of 1. *Energy Environ. Sci.* 12, 2685–2696. doi:10.1039/C9EE00734B

Tilley, S. D. (2019). Recent Advances and Emerging Trends in Photo-Electrochemical Solar Energy Conversion. *Adv. Energy Mat.* 9, 1802877. doi:10.1002/aenm.201802877

Wang, Y., Liu, J., Wang, Y., Wang, Y., and Zheng, G. (2018). Efficient Solar-Driven Electrocatalytic CO2 Reduction in a Redox-Medium-Assisted System. *Nat. Commun.* 9, 5003. doi:10.1038/s41467-018-07380-x

White, J. L., Baruch, M. F., Pander, J. E., III, Hu, Y., Fortmeyer, I. C., Park, J. E., et al. (2015). Light-driven Heterogeneous Reduction of Carbon Dioxide: Photocatalysts and Photoelectrodes. *Chem. Rev.* 115, 12888–12935. doi:10.1021/acs.chemrev.5b00370

Xiao, Y., Qian, Y., Chen, A., Qin, T., Zhang, F., Tang, H., et al. (2020). An Artificial Photosynthetic System with CO_2-reducing Solar-To-Fuel Efficiency Exceeding 20. *J. Mat. Chem. A* 8, 18310–18317. doi:10.1039/D0TA06714H

Xue, F., Si, Y., Wang, M., Liu, M., and Guo, L. (2019). Toward Efficient Photocatalytic Pure Water Splitting for Simultaneous H2 and H2O2 Production. *Nano Energy* 62, 823–831. doi:10.1016/j.nanoen.2019.05.086

Young, J. L., Steiner, M. A., Döscher, H., France, R. M., Turner, J. A., and Deutsch, T. G. (2017). Direct Solar-To-Hydrogen Conversion via Inverted Metamorphic Multi-Junction Semiconductor Architectures. *Nat. Energy.* 2, 17028. doi:10.1038/nenergy.2017.28

Zhang, H., Chen, Y., Wang, H., Wang, H., Ma, W., Zong, X., et al. (2020). Carbon Encapsulation of Organic-Inorganic Hybrid Perovskite toward Efficient and Stable Photo-Electrochemical Carbon Dioxide Reduction. *Adv. Energy Mat.* 10, 2002105. doi:10.1002/aenm.202002105

Zheng, L., Wang, J., Xuan, Y., Yan, M., Yu, X., Peng, Y., et al. (2019). A Perovskite/silicon Hybrid System with a Solar-To-Electric Power Conversion Efficiency of 25.5%. *J. Mat. Chem. A* 7, 6479–26489. doi:10.1039/C9TA10712F

Zhou, L. Q., Ling, C., Zhou, H., Wang, X., Liao, J., Reddy, G. K., et al. (2019). A High-Performance Oxygen Evolution Catalyst in Neutral-pH for Sunlight-Driven CO2 Reduction. *Nat. Commun.* 10, 4081. doi:10.1038/s41467-019-12009-8

Zhou, X., Liu, R., Sun, K., Chen, Y., Verlage, E., and Francis, S. A. (2016). Solar-driven Reduction of 1 Atm of CO_2 to Formate at 10% Energy-Conversion Efficiency by Use of a TiO_2-Protected III-V Tandem Photoanode in Conjunction with a Bipolar Membrane and a Pd/C Cathode. *ACS Energy Lett.* 1, 764–770. doi:10.1021/acsenergylett.6b00317

Conflict of Interest: The authors declare that the research was conducted in the absence of any commercial or financial relationships that could be construed as a potential conflict of interest.

Publisher's Note: All claims expressed in this article are solely those of the authors and do not necessarily represent those of their affiliated organizations, or those of the publisher, the editors and the reviewers. Any product that may be evaluated in this article, or claim that may be made by its manufacturer, is not guaranteed or endorsed by the publisher.

Copyright © 2022 Zhang, Ye, Duan, Feng, Liu and Li. This is an open-access article distributed under the terms of the Creative Commons Attribution License (CC BY). The use, distribution or reproduction in other forums is permitted, provided the original author(s) and the copyright owner(s) are credited and that the original publication in this journal is cited, in accordance with accepted academic practice. No use, distribution or reproduction is permitted which does not comply with these terms.